Organic & Biomolecular Chemistry

ROYAL SOCIETY OF CHEMISTRY

PAPER

View Article Online
View Journal

Cite this: DOI: 10.1039/d2ob00175f

Fluorogenic monomer activation for protein-initiated atom transfer radical polymerization†

Danyal Tahseen, Jemima R. Sackey-Addo, Zachary T. Allen, Joseph T. Anderson, Jordan B. McMurry and Christina B. Cooley *

Fluorogenic atom transfer radical polymerization (ATRP) directly detects initiator-dependent polymer formation, as initially non-fluorescent polycyclic aromatic probe monomers reveal visible fluorescence upon polymerization in real time. Advancement of this initial proof-of-concept toward biodetection applications requires both a more detailed mechanistic understanding of probe fluorescence activation, and the ability to initiate fluorogenic polymerization directly from a biomolecule surface. Here, we show that simple monomer hydrogenation, independent of polymerization, reveals probe fluorescence, supporting the critical role of covalent enone attachment in fluorogenic probe quenching and subsequent fluorescence activation. We next demonstrate bioorthogonal, protein-initiated fluorogenic ATRP by the surface conjugation and characterization of protein–initiator conjugates of a model protein, bovine serum albumin (BSA). Fluorogenic ATRP from initiator-modified protein allows for real-time visualization of polymer formation with negligible background fluorescence from unmodified BSA controls. We further probe the bioorthogonality of this fluorogenic ATRP assay by assessing polymer formation in a complex biological environment, spiked with fetal bovine serum. Taken together, we demonstrate the potential of aqueous fluorogenic ATRP as a robust, bioorthogonal method for biomolecular-initiated polymerization by real-time fluorescence activation.

Received 27th January 2022,
Accepted 6th June 2022

DOI: 10.1039/d2ob00175f

rsc.li/obc

Introduction

The sensitive detection of biomolecular analytes is crucial to disease diagnosis and treatment, relying on specific discrimination of desired biomolecules from a complex biological environment followed by amplification of that discrete molecular interaction into a macro, detectable signal.[1] Radical polymerization has emerged as a chemical approach to signal amplification as a single initiation event enables growth of a long polymer chain. By coupling polymerization initiators to analytes of interest, the detection of synthesized polymer by various methods has enabled the sensitive detection of biomolecules including DNA and proteins.[2–18] However, many of the polymer detection methods to date rely on pre- or post-polymerization steps to read out for formation of synthesized polymer in a qualitative, on–off fashion, motivating the exploration of alternative approaches to directly and quantitatively monitor polymerization progress.

We have recently developed a simple, real-time fluorescence method for signal amplification and analyte detection in aqueous media by fluorogenic atom transfer radical polymerization (ATRP).[19] In this approach, non-fluorescent, "dark" polycyclic aromatic probe monomers become fluorescent when incorporated into an actively propagating polymer chain, contingent upon an initiation event. ATRP was chosen as a well-controlled and robust polymerization method[20–25] that allowed for quantitative, small-molecule analyte detection by visible fluorescence as a function of initiator concentration.[19]

Specific activation of quenched pyrene, anthracene or acridine methacrylamide probe monomers upon polymerization enables fluorescence detection of polymer synthesis, with the monomers postulated to be non-fluorescent due to covalent attachment of the α,β-unsaturated amide.[19,26–28] For example, the non-covalent addition of enones such as acrylamide and succinimide to polycyclic aromatic hydrocarbon probes in solution can function as partial quenchers of fluorescence by electron transfer.[29] Initial explorations of this class of fluorogenic monomer probes such as fluorene methacrylate[30] and pyrene maleimide[31] derivatives further demonstrate that as the enone functionality is first covalently coupled then moved closer to the fluorophore itself, complete quenching of probe fluorescence is observed.[26] Upon polymerization and saturation of the C=C double bonds in these various monomer scaffolds, probe fluorescence is revealed. Although these

Department of Chemistry, Trinity University, 1 Trinity Place, San Antonio, TX 78212, USA. E-mail: ccooley@trinity.edu

† Electronic supplementary information (ESI) available. See DOI: https://doi.org/10.1039/d2ob00175f

observations support the hypothesis that fluorescence activation is solely due to removal of the enone quencher upon polymerization, this effect has thus far only been studied in the context of polymer formation. However, polymer synthesis in solution affects multiple additional variables known to affect pyrene and anthracene probe fluorescence, including local concentration, dielectric constant, and potential aggregation and excimer formation,[32,33] motivating further studies to probe the mechanism of fluorogenic monomer activation. Here, we provide additional support for the enone quenching hypothesis of monomer fluorescence activation, demonstrating that hydrogenation of pyrene methacrylamide reveals fluorescence independent of polymerization.

To advance the fluorogenic ATRP method as a viable signal amplification strategy for biomolecular detection, we further sought to initiate fluorogenic ATRP directly from a modified protein surface in a bioorthogonal manner. Utilizing bovine serum albumin (BSA) as a model protein bioanalyte, we synthesized BSA–initiator conjugates with varying degrees of modification that retained their protein fold by circular dichroism (CD) spectroscopy. Fluorogenic ATRP from modified BSA initiators showed increasing fluorescence with polymerization reaction time and negligible background fluorescence from unmodified BSA controls. We further probed the biorthogonality of this fluorogenic ATRP assay by assessing polymer fluorescence in a complex biological environment, spiked with fetal bovine serum. This work establishes fluorogenic ATRP as capable of biomolecule-initiated fluorescence activation, motivating the continued development of fluorogenic polymerization for biosensor applications.

Experimental section

Pyrene monomer hydrogenation

Pyrene methacrylamide **1**[19] (40 mg, 0.14 mmol) was dissolved in 10 mL of THF. An aliquot (3 mL) of this solution was transferred to a cuvette and observed for fluorescence by fluorimeter emission scans and photographs after irradiation by long-wave UV light. Following transfer of the aliquot back into the round bottom flask, 10% Pd/C (15 mg, 0.14 mmol) was added to the solution. Hydrogen gas (H_2) was bubbled through the solution for 1 h at rt. A 3 mL aliquot was again removed for fluorescence measurements. Full conversion of starting material to the reduced product was observed by TLC (9 : 1 CH_2Cl_2 : hexanes).

Protein–initiator conjugate synthesis

N-Hydroxysuccinimidyl ester **3**[34] (1.0 g, 5.5 mmol) was dissolved in 2 mL of DMSO and sonicated. Unmodified **BSA** (1.0 g, 0.5 mmol lysine residues) was dissolved in 500 mL of 0.1 M PBS (pH 7.4) and the DMSO solution containing **3** was added dropwise. The reaction was stirred for 18 h at rt, then purified by centrifugal filtration in Centricon Plus-20 centrifugal dialysis-filtration tubes with a 30 kDa cutoff membrane. Each aliquot was washed 4× with deionized water, then eluted with 0.5 mL H_2O. Aliquots were combined, protein concentrations determined by Nanodrop, and diluted with water to provide 100 mM (4 mg mL^{-1}) protein stock solutions of **M-BSA** (11 initiator equivalents per lysine). The reaction was performed similarly with a reduction in amount of NHS ester **3** (0.5 g, 2.75 mmol) to afford **M-BSA** with 5.5 initiator equivalents per lysine. In all cases, total protein recovery was >90%.

Protein folding analysis by circular dichroism

Protein solutions (**BSA**, **M-BSA** with 5.5 or 11 initiator equivalents per lysine) in water were diluted with PBS buffer (pH 7.4) to prepare samples with final protein concentrations of 0.05 mg mL^{-1} (total volume 0.350 mL). A guanidinium hydrochloride (Gdn-HCl) solution was prepared (8 M in PBS pH 7.4). Denatured protein samples were accessed by mixing **BSA** (0.05 mg mL^{-1}) and Gdn-HCl (7 M), adding PBS as necessary for a total volume per sample of 0.350 mL. The samples were equilibrated for 1 h at rt before circular dichroism (CD) spectral analysis with a Jasco J-815 spectrophotometer. Spectra were collected at 25 °C from 250 to 200 nm with a scan speed of 20 nm min^{-1}, a bandwidth of 1 nm, a resolution of 1 nm, a response time of 1 s, and a cycle time of 2 min.

Protein-initiated fluorogenic ATRP

Fluorogenic ATRP reactions from a protein surface were conducted with slight modifications from fluorogenic ATRP small-molecule methods.[19] **BSA** or **M-BSA** proteins (0.006 mmol, 60 μL of 100 mM stock solution in water) were combined with PEG methacrylate monomer **4** (0.7043 g, 1.5 mmol), sodium chloride (NaCl, 17.4 mg, 0.3 mmol), stock solutions of 25 mM copper bromide ($CuBr_2$) and 200 mM tris(2-pyridylmethyl) amine (TPMA) in water (6 μL, final concentrations 0.15 μmol $CuBr_2$ and 1.2 μmol TPMA) and a 5 mM stock solution of fluorogenic methacrylamide anthracene monomer **5** in water with 366 mM sodium dodecyl sulfate (SDS, 0.300 mL, final concentrations 0.150 mmol monomer **5**, 0.102 mmol SDS). Deionized water was added to give a final volume of 2.30 mL in a round-bottom flask. DMF was added (0.03 mL) as an internal standard for monitoring the reaction by ^{1}H NMR. The flask was sealed and purged with nitrogen bubbling through the solution for 30–60 min, and then the solution was transferred to a sealed quartz cuvette containing a stir bar and placed in a 30 °C oil bath under nitrogen. A 16 mM ascorbic acid solution in water was separately purged with nitrogen for 30–60 min, then 0.090 mL (1.4 μmol) was slowly added to the cuvette to start the reaction. At various times, the cuvettes were removed from the oil bath and examined for fluorescence by fluorimeter emission scans and/or photographs after irradiation by long-wave UV light. After 1 h, an additional 0.090 mL (1.4 μmol) of degassed ascorbic acid solution was added and the reaction continued to be monitored for up to 24 h. In select cases, the synthesized polymers were cleaved from the protein by adding 200 μL of the reaction mixture to 200 μL of 5% KOH solution for 2 h at room temperature, then diluted in THF and analyzed by gel permeation chromatography (GPC).

For experiments probing the bioorthogonality of the assay, fluorogenic ATRP reactions were performed as described above with the addition of 80 μL fetal bovine serum (FBS, Omega Scientific) into the polymerization mixture.

Results and discussion

Monomer hydrogenation activates probe fluorescence

To explore whether the α,β-unsaturation of the methacrylamide is solely responsible for quenching monomer fluorescence in the absence of polymer formation, we analyzed the fluorescence before and after palladium-catalyzed hydrogenation of pyrene methacrylamide monomer **1** (Fig. 1). Pyrene monomer **1** was chosen for this experiment as the fluorescence properties of pyrene are particularly sensitive to aggregation and environmental changes, and pyrene is used widely in polymer, protein and nucleic acid labelling studies.[33,35,36] Palladium-catalyzed hydrogenation of pyrene methacrylamide **1** in organic solvent, THF, affords clean conversion to the reduced derivative **2** after 1 h (Fig. 1a). Fluorescence measurements pre- and post-hydrogenation system demonstrate that pyrene fluorescence is fully quenched in the intact monomer form, but clearly revealed upon hydrogenation (Fig. 1b). Our results from this simplified system, excluding all other variables which may change during the course of a polymerization reaction, demonstrate that probe fluorescence can be activated exclusively by C=C bond saturation, and bolster the hypothesis that removal of the covalent enone quencher upon polymerization is the primary driver of fluorescence activation in this family of fluorogenic monomer probes.

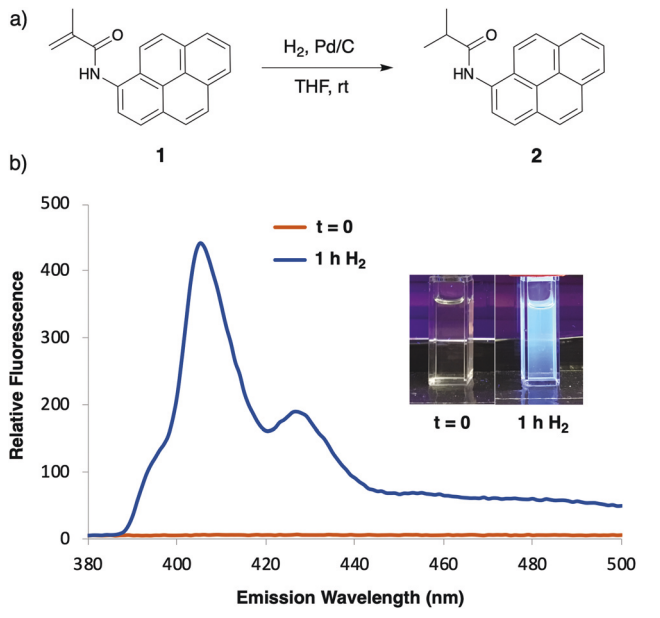

Fig. 1 (a) Hydrogenation reaction conditions for the conversion of pyrene methacrylamide 1 to the reduced pyrene derivative 2. (b) Emission spectra and photographs of aliquots of the reaction in (a) at the indicated reaction times following a 337 nm excitation.

Synthesis and characterization of protein–initiator conjugates

We next sought to initiate fluorogenic ATRP directly from a bioanalyte surface. Utilizing bovine serum albumin (BSA) as a model protein and bioanalyte, we synthesized protein–initiator conjugate(s) as shown in Scheme 1. ATRP-initiator *N*-hydroxysuccinimidyl ester conjugate **3** was synthesized as previously described,[34] then reacted non-specifically with the surface lysine residues of **BSA** under buffered conditions. We varied the initiator : protein reaction ratio in order to access modified BSA initiator conjugates (**M-BSA**) with two differing degrees of modification, in an effort to explore how initiator modification affects resulting protein–initiator conjugate properties. **M-BSA** conjugates were synthesized as shown in Scheme 1 with either 5.5 or 11 equivalents of **3** in solution relative to BSA lysine residues.

Characterization of the **M-BSA** conjugates by mass spectrometry indicated that the number of initiator modifications increases with the amount of **3** in solution (Fig. S1†). Relative to unmodified, control **BSA** (subjected to identical reaction conditions sans **3** treatment), **M-BSA** with 5.5 equivalents **3** per BSA lysine demonstrated a mass increase consistent with 23–-24 modifications per protein. **M-BSA** with 11 equivalents provided a mass increase consistent with 37–38 modifications. Due to the non-specific nature of conjugation, the **M-BSA** conjugates also exhibited increased heterogeneity as a function of increased initiator modification, as observed by peak broadening. Analytical LC-MS analysis of unmodified **BSA** and the **M-BSA** conjugates further demonstrated a reduction in surface polarity and an increase in heterogeneity as a function of initiator modification, with no detectable unreacted initiator in the purified samples (Fig. S2†).

Protein–initiator conjugates retain protein fold and structure

It is desirable for the initiator-modified protein to retain its native fold following initiator conjugation, in order to preserve target binding interactions and to enable relevant diagnostic applications of protein-initiated, fluorogenic polymerization. We therefore sought next to evaluate the native, folded conformation of the synthesized **M-BSA** conjugates by circular dichroism (CD) spectroscopy (Fig. 2).

Unmodified, control **BSA** in its native form (N) exhibits a signature, primarily alpha-helical CD spectrum that disappears upon denaturation with guanidinium-HCl (D). Gratifyingly, the maximally modified **M-BSA** (11 equivalents per BSA lysine) provides a similar CD spectrum to the native **BSA**, indicating that

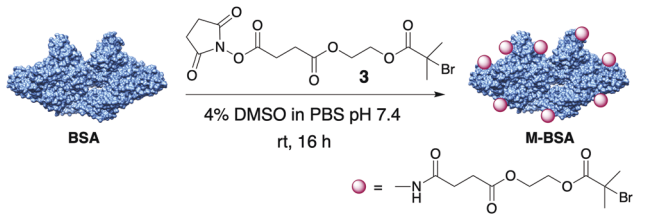

Scheme 1 Synthesis of ATRP initiator protein conjugate **M-BSA**.

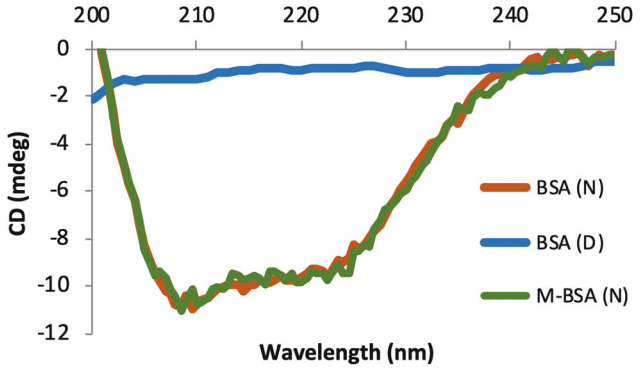

Fig. 2 Circular dichroism (CD) spectra of unmodified BSA (native (N) and denatured (D) by 7 m Gdn-HCl) and maximally modified, native **M-BSA** (11 equivalents of initiator per BSA lysine upon conjugation).

surface modification under the reaction conditions in Scheme 1 does not lead to unfolding of the protein (Fig. 2). In a similar fashion, the 5.5 equivalents **M-BSA** conjugate also retains a native fold by CD analysis (Fig. S3†). Taken together, these results verify that surface modification of **BSA** with small molecule ATRP initiators do not affect the protein fold, and suggests the preservation of relevant binding interactions if desired for subsequent downstream applications.

Fluorogenic ATRP from modified protein surface

Following the synthesis and characterization of the model initiator–protein **M-BSA** conjugates, we next subjected the **M-BSA** conjugate to fluorogenic ATRP reaction conditions[19] to investigate whether the polymer could be grafted directly from a protein surface with concomitant detectable fluorescence (Scheme 2 and Fig. 3). **M-BSA** (5.5 equivalents per BSA lysine) was used as the ATRP initiator with PEG monomer **4** and anthracene fluorogenic monomer **5** under aqueous ATRP conditions[19,37] to generate a fluorescent, water-soluble, protein–polymer hybrid.

Monitoring fluorescence at various time points demonstrates that the monomers in solution are initially non-fluorescent, with fluorescence growing in over time as the protein–polymer conjugate is formed (Fig. 3). Visible fluorescence is observable in as little as 2 h of reaction time, with the reaction reaching maximum fluorescence at 24 h. Unmodified **BSA**

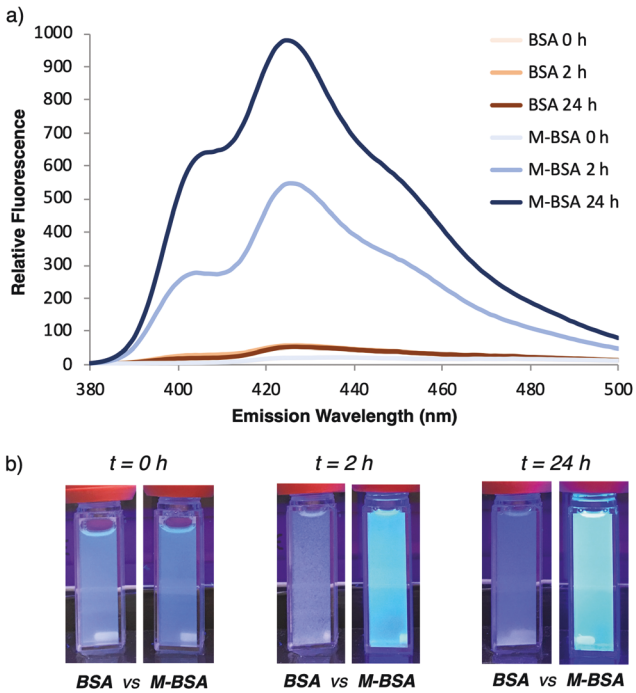

Fig. 3 (a) Fluorescence emission spectra for the protein-initiated fluorogenic ATRP reaction shown in Scheme 2 (initiated by **M-BSA**, 5.5 equivalents initiator per BSA lysine) or with unmodified BSA as the protein component at indicated times following 371 nm excitation. (b) Photographs of the reactions at indicated times illuminated by a hand-held UV light (365 nm).

gives no observable background fluorescence during the entire 24 h of reaction time, indicating that polymer formation and fluorescence generation is specific to the initiator-modified conjugate and compatible with a wide variety of functional groups observed in protein side chains. Similar results were observed for the maximally functionalized polymer **M-BSA** (11 equivalents per BSA lysine, Fig. S4†), with bright visible fluorescence at 24 h specifically from **M-BSA**-initiated polymer formation. Synthesized polymers were cleaved from the protein by incubation with 5% KOH[34] and analyzed by GPC. Polymer formation was detected only under the **M-BSA** polymerization conditions (M_n = 57 300, M_w/M_n = 1.488), with the relatively broadened dispersity reflecting the heterogeneity of non-selective protein surface modification.

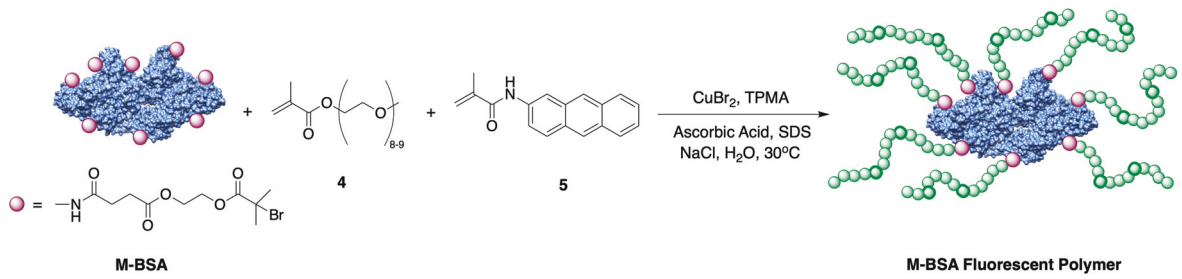

Scheme 2 Fluorogenic ATRP conditions initiating from **M-BSA**.

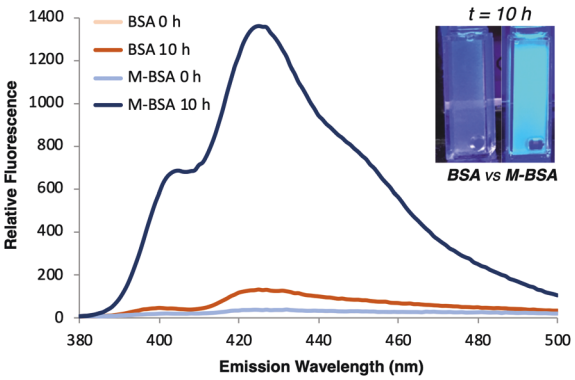

Fig. 4 Fluorescence emission spectra and photographs of the protein-initiated fluorogenic ATRP reaction in Scheme 2, spiked with FBS (3.5%). Emission spectra and photos were taken at indicated times following a 371 nm excitation or hand-held UV lamp irradiation.

Bioorthogonality of fluorogenic protein-initiated ATRP

To further explore the functional group tolerability and ability to conduct protein-initiated, fluorogenic ATRP in a complex biological environment, we performed the fluorogenic ATRP reaction shown in Scheme 2 in the presence of added fetal bovine serum (FBS, 3.5% total reaction volume, Fig. 4). FBS contains a complex array of proteins, in addition to significantly higher concentrations of unmodified **BSA**. Fig. 4 demonstrates that even in a complex biological mixture with high protein concentrations, polymer formation and visibly bright fluorescence were observable within 10 h of reaction time with initiator-modified **M-BSA**. Under these conditions, slightly detectable levels of background fluorescence from unmodified **BSA** were observable by fluorescence quantitation (although not by eye) under the same reaction time. However, fluorescence emission and visual analysis allowed for discrimination between unmodified and modified BSA, even against the complex fluid mixture of biomolecules in FBS. Although this technique is currently limited to initiation from previously synthesized protein–initiator conjugates, the ability to observe polymerization-dependent fluorescence activation in a biorthogonal fashion provides support for the ongoing development and application of fluorogenic polymerization for the detection of biomolecules and biomolecular recognition events.

Conclusions

We have advanced fluorogenic ATRP here by validating the proposed mechanism of monomer fluorescence activation, and applying it to initiation directly from a biomolecule surface. Fluorogenic monomer hydrogenation demonstrated that removal of α,β-unsaturation is solely responsible for the probe fluorescence activation observed upon polymerization. Moving toward biomolecular-initiated applications, we first synthesized model BSA protein-initiator conjugates, accessible in a controllable fashion while retaining the protein's native conformation. Modified protein–initiator conjugates were reacted under fluorogenic ATRP conditions, with visual fluorescence increasing with polymerization reaction time. Protein–polymer hybrid formation and fluorescence were specific to the initiator-modified protein, even in the context of complex biological mixtures. This study moves us closer to our goal of applying this fluorogenic polymerization approach to the direct detection of modified biomolecules or their binding partners in solution. Further studies to optimize the fluorogenic polymerization reaction by improving the reaction kinetics and biodetection applications of this method are ongoing and will be reported in due course.

Conflicts of interest

There are no conflicts to declare.

Acknowledgements

We gratefully acknowledge Wendell Griffith and the mass spectrometry core facility at the University of Texas San Antonio for assistance with protein–initiator conjugate characterization. Acknowledgment is made to the Donors of the American Chemical Society Petroleum Research Fund for support of this research. This work was further supported by the Welch Foundation (W-1984 and W-0031), the National Science Foundation (CHE-1726441 and CHE-2045398), the San Antonio Area Foundation, and Trinity University.

References

1 M. Urdea, L. A. Penny, S. S. Olmsted, M. Y. Giovanni, P. Kaspar, A. Shepherd, P. Wilson, C. A. Dahl, S. Buchsbaum, G. Moeller and D. C. Hay Burgess, *Nature*, 2006, **444**, 73–79.
2 K. Kaastrup and H. D. Sikes, *Chem. Soc. Rev.*, 2016, **45**, 532–545.
3 H. Qian and L. He, *Sens. Actuators, B*, 2010, **150**, 594–600.
4 H. D. Sikes, R. R. Hansen, L. M. Johnson, R. Jenison, J. W. Birks, K. L. Rowlen and C. N. Bowman, *Nat. Mater.*, 2007, **7**, 52–56.
5 R. R. Hansen, H. D. Sikes and C. N. Bowman, *Biomacromolecules*, 2008, **9**, 355–362.
6 H. D. Sikes, R. Jenison and C. N. Bowman, *Lab Chip*, 2009, **9**, 653–656.
7 Y. Liu, Y. Dong, J. Jauw, M. J. Linman and Q. Cheng, *Anal. Chem.*, 2010, **82**, 3679–3685.
8 A. K. Badu-Tawiah, S. Lathwal, K. Kaastrup, M. Al-Sayah, D. C. Christodouleas, B. S. Smith, G. M. Whitesides and H. D. Sikes, *Lab Chip*, 2015, **15**, 655–659.
9 K. Kaastrup and H. D. Sikes, *Lab Chip*, 2012, **12**, 4055–4054.
10 Y. Wu, S. Liu and L. He, *Anal. Chem.*, 2009, **81**, 7015–7021.
11 Y. Wu, W. Wei and S. Liu, *Acc. Chem. Res.*, 2012, **45**, 1441–1450.

12 Y. Wu, P. Xue, K. M. Hui and Y. Kang, *Biosens. Bioelectron.*, 2014, **52**, 180–187.
13 A. J. Gormley, R. Chapman and M. M. Stevens, *Nano Lett.*, 2014, **14**, 6368–6373.
14 L. Zhang, W. Zhao, X. Liu, G. Wang, Y. Wang, D. Li, L. Xie, Y. Gao, H. Deng and W. Gao, *Biomaterials*, 2015, **64**, 2–9.
15 B. J. Berron, L. M. Johnson, X. Ba, J. D. McCall, N. J. Alvey, K. S. Anseth and C. N. Bowman, *Biotechnol. Bioeng.*, 2011, **108**, 1521–1528.
16 X. Zheng, L. Zhao, D. Wen, X. Wang, H. Yang, W. Feng and J. Kong, *Talanta*, 2020, **207**, 120290.
17 L. Zhao, H. Yang, X. Zheng, J. Li, L. Jian, W. Feng and J. Kong, *Biosens. Bioelectron.*, 2020, **150**, 111895.
18 S. Kim and H. D. Sikes, *Polym. Chem.*, 2020, **11**, 1424–1444.
19 Z. T. Allen, J. R. Sackey-Addo, M. P. Hopps, D. Tahseen, J. T. Anderson, T. A. Graf and C. B. Cooley, *Chem. Sci.*, 2019, **10**, 1017–1022.
20 J.-S. Wang and K. Matyjaszewski, *J. Am. Chem. Soc.*, 1995, **117**, 5614–5615.
21 T. E. Patten, J. Xia, T. Abernathy and K. Matyjaszewski, *Science*, 1996, **272**, 866–868.
22 K. Matyjaszewski and J. Xia, *Chem. Rev.*, 2001, **101**, 2921–2990.
23 K. Matyjaszewski, *Macromolecules*, 2012, **45**, 4015–4039.
24 K. Matyjaszewski and N. V. Tsarevsky, *J. Am. Chem. Soc.*, 2014, **136**, 6513–6533.
25 C. Boyer, N. A. Corrigan, K. Jung, D. Nguyen, T.-K. Nguyen, N. N. M. Adnan, S. Oliver, S. Shanmugam and J. Yeow, *Chem. Rev.*, 2016, **116**, 1803–1949.
26 M. S. Frahn, R. D. Abellon, W. F. Jager, L. H. Luthjens and J. M. Warman, *Nucl. Instrum. Methods Phys. Res., Sect. B*, 2001, **185**, 241–247.
27 M. S. Frahn, L. H. Luthjens and J. M. Warman, *Polymer*, 2003, **44**, 7933–7938.
28 M. S. Frahn, R. D. Abellon, L. H. Luthjens, M. J. W. Vermeulen and J. M. Warman, *Nucl. Instrum. Methods Phys. Res., Sect. B*, 2003, **208**, 405–410.
29 M. R. Eftink, T. J. Selva and Z. Wasylewski, *Photochem. Photobiol.*, 1987, **46**, 23–30.
30 K. E. Miller, E. L. Burch, F. D. Lewis and J. M. Torkelson, *J. Polym. Sci., Part B: Polym. Phys.*, 1994, **32**, 2625–2635.
31 J. M. Warman, R. D. Abellon, H. J. Verhey, J. W. Verhoeven and J. W. Hofstraat, *J. Phys. Chem. B*, 1997, **101**, 4913–4916.
32 S. P. Kozel, Y. Y. Gotlib, G. I. Lashkov and N. S. Shelekhov, *Polym. Sci. USSR*, 1982, **24**, 1578–1585.
33 F. M. Winnik, *Chem. Rev.*, 1993, **93**, 587–614.
34 S. Averick, A. Simakova, S. Park, D. Konkolewicz, A. J. D. Magenau, R. A. Mehl and K. Matyjaszewski, *ACS Macro Lett.*, 2012, **1**, 6–10.
35 G. Bains, A. B. Patel and V. Narayanaswami, *Molecules*, 2011, **16**, 7909–7935.
36 J. Huang, Y. Wu, Y. Chen, Z. Zhu, X. Yang, C. J. Yang, K. Wang and W. Tan, *Angew. Chem., Int. Ed.*, 2010, **50**, 401–404.
37 A. Simakova, S. E. Averick, D. Konkolewicz and K. Matyjaszewski, *Macromolecules*, 2012, **45**, 6371–6379.